ACS APPLIED MATERIALS & INTERFACES

www.acsami.org

Research Article

Shining Light on Cyclopentadienone–Norbornadiene Diels–Alder Adducts to Enable Photoinduced Click Chemistry with Cyclopentadiene

Sophia J. Bailey, Friedrich Stricker, Erik Hopkins, Maxwell Z. Wilson, and Javier Read de Alaniz*

Cite This: *ACS Appl. Mater. Interfaces* 2021, 13, 35422–35430

Read Online

ACCESS | Metrics & More | Article Recommendations | Supporting Information

ABSTRACT: A new Diels–Alder (DA)-based photopatterning platform is presented, which exploits the irreversible, light-induced decarbonylation and subsequent cleavage of cyclopentadienone–norbornadiene (CPD–NBD) adducts. A series of CPD–NBD adducts have been prepared and systematically studied toward the use in a polymeric material photopatterning platform. By incorporating an optimized CPD–NBD adduct into polymer networks, it is demonstrated that cyclopentadiene may be unveiled upon 365 nm irradiation and subsequently clicked to a variety of maleimides with spatial control under mild reaction conditions and with fast kinetics. Unlike currently available photoinduced Diels–Alder reactions that rely on trapping transient, photocaged dienes, this platform introduces a persistent, yet highly reactive diene after irradiation, enabling the use of photosensitive species such as cyanine dyes to be patterned. To highlight the potential use of this platform in a variety of material applications, we demonstrate two proof-of-concepts: patterned conjugation of multiple dyes into a polyacrylate network and preprogrammed ligation of streptavidin into poly(ethylene glycol) hydrogels.

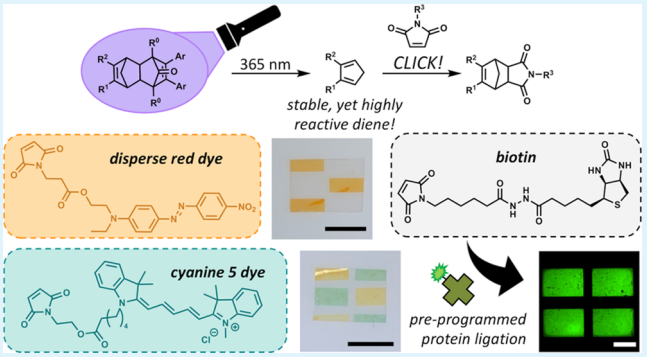

KEYWORDS: *click chemistry, Diels–Alder, cyclopentadiene, photochemistry, photopatterning*

1. INTRODUCTION

The well-defined incorporation of functional molecules into polymer networks is an attractive endeavor with promise throughout materials science. With regard to biomaterials, the introduction of biologically relevant small molecules and proteins within synthetic hydrogels has numerous applications including adhesion,[1] drug delivery,[2] and tissue engineering;[3] whereas, in the field of smart materials, a multitude of stimuli-responsive molecules have been exploited within polymer networks such as liquid crystals,[4] photothermal agents,[5] and photoswitches.[6,7] Introducing these agents into polymer networks typically relies on noncovalent blending or the use of functionalized monomers, both resulting in bulk incorporation throughout the network. Of particular interest, however, is the high-resolution spatial control over chemical functionalization, offering significant advantages in the microfabrication of materials varying from sequentially responsive actuators[8−10] to patterned cell microenvironments.[11−13] Successful preparation of these materials is dependent on identifying chemistries that offer spatial control while remaining highly efficient, mild, and compatible with numerous functionalities and biological systems.

Diels–Alder (DA) cycloadditions are a distinguished click chemistry[14] that have been extensively employed throughout organic synthesis, materials science, and bioconjugation. Unlike other common click chemistries, such as the copper-(I)-catalyzed alkyne–azide cycloaddition,[15] thiol–Michael,[16] or thiol–ene,[17] which rely on toxic copper catalysis, additives, or radicals, DA cycloadditions offer a mild, additive-free approach while maintaining high efficiency, tunable kinetics, functional group tolerance, and bio-orthogonality. In polymer chemistry, DA cycloadditions have served as the basis of a number of block copolymer "click" reactions,[18−23] and the reversibility of the DA reaction has served as a platform for the preparation of thermally re-mendable polymer networks.[24−26] Within biomaterials, the fast and bio-orthogonal nature of the inverse electron demand Diels–Alder (IEDDA) cycloaddition has led to the development of a new bioconjugation platform[27] and numerous approaches to protein modification through IEDDA.[28] Normal-demand DA cycloadditions have also been successfully demonstrated in biological systems by developing strategies to enable the use of more reactive diene and

Received: May 10, 2021
Accepted: July 12, 2021
Published: July 26, 2021

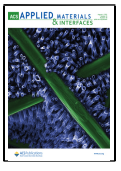

dienophile partners for the preparation of antibody−drug conjugates[29,30] and rapid 3D cell encapsulation.[31]

Given the highly efficient, mild, and additive-free nature of DA cycloadditions, efforts have been made to further extend the utility of these reactions through temporal and spatial control. The development of photocaged dienes has offered significant advances in obtaining such control in material systems. The photoenolization of *o*-substituted benzophenones was first presented in 1961,[32] and the use of such photocaged dienes was introduced to polymer chemistry by Meador et al. in 1996 (Figure 1a).[33] More recently, photoenolization of *o*-

Scheme 1. (a) Traditional Photocaged Dienes Can Be Photoactivated and Undergo an In Situ DA Click Reaction and (b) the Phototriggered Cleavage of Norbornadiene−Cyclopentadienone Adducts to Cyclopentadiene Allows for Either In Situ or Postirradiation DA Click Reaction with a Variety of Functional Maleimides

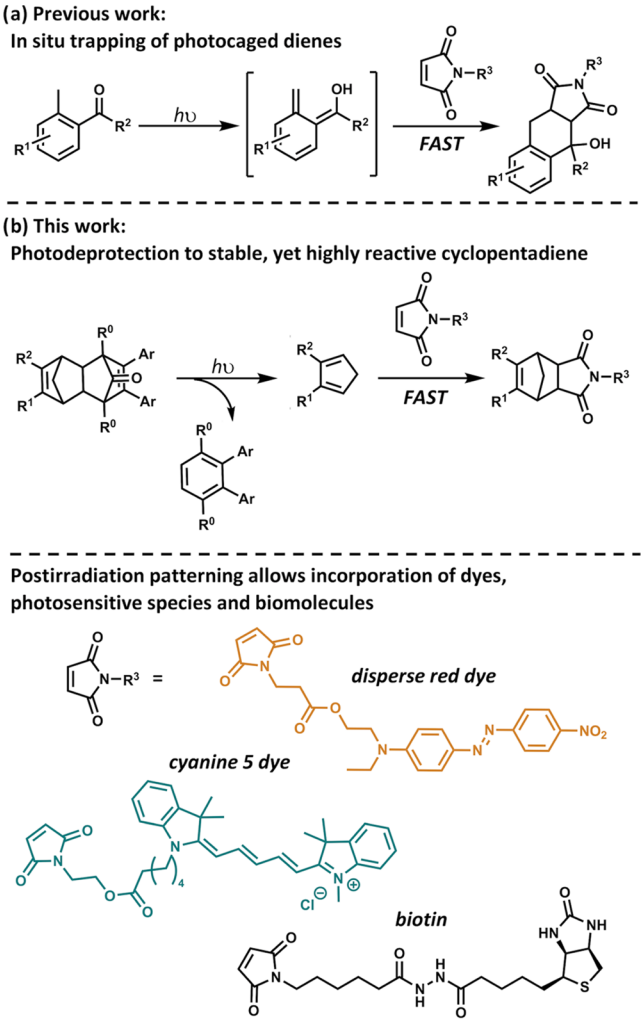

methylbenzaldehydes (*o*-MBAs) to *o*-quinodimethanes (*o*-QDMs) has been employed in a number of DA systems by Barner-Kowollik and co-workers, including the click coupling of block copolymers[34,35] and the functionalization of (bio)-surfaces.[36−38] In addition, the photochemical dehydration of 3-hydroxy-2-naphthalenemethanol derivatives has offered an alternative route to highly reactive diene intermediates.[39] Additionally, photogenerated dienophiles have also been

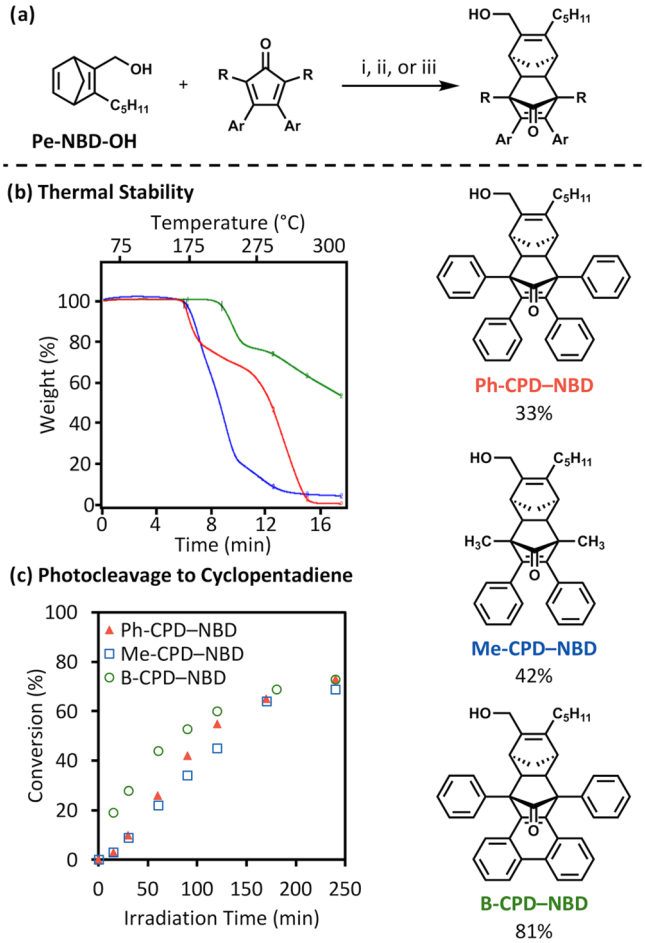

Figure 1. (a) (i) Ph-CPD (2.0 equiv), chloroform, 75 °C, 5 days, 33% yield of Ph-CPD−NBD; (ii) Me-CPD (1.5 equiv), toluene, 85 °C, 24 h, 42% yield of Me-CPD−NBD; (iii) B-CPD (1.1 equiv), toluene, 70 °C, 18 h, 81% yield of B-CPD−NBD. (b) Thermogravimetric analysis of Ph-CPD−NBD (red trace), B-CPD−NBD (green trace), and Me-CPD−NBD (blue trace) at a ramp of 20 °C/min from room temperature to 300 °C. (c) Conversion to Cp upon irradiation of 25 mM solution of each adduct at 300 nm determined by ^{1}H nuclear magnetic resonance (NMR) over 240 min.

investigated for block copolymer synthesis[40] and surface functionalization by photolysis of phenacyl sulfides followed by hetero-DA reactions.[41] Light has also been used to "gate" the reversibility of the DA reaction through the use of dithienylethene and dithienylfuran photoswitching systems.[42,43] The disadvantage to the currently available photogenerated diene systems, however, is the short lifetimes of the diene intermediates, requiring the in situ trapping with a dienophile. Because UV light is required for the photodeprotection in these systems,[34−39,41] in situ trapping is not compatible with photosensitive moieties or absorbing species required for many stimuli-responsive and biologically relevant applications. We therefore anticipate that developing an effective and efficient synthetic protocol to access highly reactive yet persistent dienes within materials will be vital to expand the potential applications of photoinduced DA cycloadditions. Importantly, the success of this goal will add to the toolbox of the so-called "photoclick" reactions[44] and will provide a complementary approach to existing methods for enabling functionalization of advanced materials with temporal and spatial control (Scheme 1).

https://doi.org/10.1021/acsami.1c08670
ACS Appl. Mater. Interfaces 2021, 13, 35422−35430

Over the recent years, our group became interested in cyclopentadiene for its reported high reactivity[45] and exploitation in polymer click reactions.[19,25,46,47] To expand the utility of this diene, we have sought to develop methods to harness the high reactivity to enable efficient bioconjugation[29] and controlled polymer click reactions.[22,48] Prompted by our recent utilization of norbornadiene-functionalized polymers as a chemically triggered precursor to Cp,[22,48] we targeted the development of a phototriggered platform, which would offer spatiotemporal control over the introduction of these highly reactive units. Inspired by reports of the photo- or thermally induced loss of carbon monoxide from bridged cyclopentadienone−norbornadiene (CPD−NBD) Diels−Alder adducts,[49−52] we envisioned that the resulting retro-DA cleavage could be exploited to obtain cyclopentadiene on demand. CPD−alkene adducts have been utilized extensively for the preparation of substituted benzenes[53,54] and have recently been employed in the preparation of CO-releasing prodrugs.[55,56] Notably, the photodecarbonylation of CPD−maleimide adducts has been utilized to pattern surfaces with nonmodified peptides by utilizing a photoactivated triphenylene imide that is susceptible to ring opening by amines.[37] The disadvantage of this clever approach, however, is the necessity for a significant excess of amine groups to achieve the imide ring opening and subsequent patterning. Irradiation of CPD−NBD adducts, on the other hand, would produce a highly reactive Cp species that readily reacts with dienophiles.[45] Furthermore, in contrast to current photoinduced Diels−Alder reactions that produce a transient diene, the loss of CO and formation of thermodynamically stable aromatic byproduct results in an irreversible reaction, allowing for the persistence of stable Cp units in the material until treatment with the dienophile of choice. A similar approach is used in the irreversible photochemical activation of tetrazole for nitrile imine-mediated tetrazole−ene cycloaddition (NITEC), which readily reacts with dipolarophiles.[57,58] The irreversible nature of NITEC has been demonstrated to provide much higher surface graft densities than the more transient *o*-MBA photoactivation to *o*-QDM.[59] In addition, although Cp is a highly reactive diene that can dimerize over extended storage,[22,60] it is inherently more stable than nitrile imines,[61] offering a persistent species after the cessation of irradiation. This unique feature would enable functionalization with a number of photosensitive species, as the spatially controlled Diels−Alder reaction could take place post irradiation. Moreover, this approach would also be amenable to in situ functionalization with maleimides that are stable to 365 nm irradiation, thus complementing existing approaches.

Herein, we report the use of such CPD−NBD adducts within polymer networks as photolabile Cp precursors (Figure 1b) for subsequent DA-based patterning of dyes and biomolecules. We first present a comparative study investigating the synthesis, thermal stability, and photoinduced Cp production from a series of CPD−NBD adducts; the results of this study provide an optimal candidate for utilization in patterning a variety of materials. We then outline two proof-of-concept photoclick demonstrations with maleimide-bearing molecules, biotin and two common dyes, that highlight the potential use of this platform in bio- or stimuli-responsive materials.

2. RESULTS AND DISCUSSION

2.1. Identification of the Optimal CPD−NBD Adduct.

2.1.1. Efficiency of DA with Cyclopentadienone. For utilization in various polymeric material systems, we sought to design a CPD−NBD adduct that could be prepared easily and in high yields from either commercially available or highly scalable starting materials. For this reason, we chose to explore the Diels−Alder reaction with our previously reported, highly scalable NBD derivative Pe-NBD-OH[22,48] and three commercially available cyclopentadienones (CPDs): tetraphenylcyclopentadienone (Ph-CPD), 2,5-dimethyl-3,4-diphenylcyclopentadienone (Me-CPD), and the fused analogue to Ph-CPD, 1,3-diphenylcyclopenta[*l*]phenanthren-2-one (B-CPD). To investigate the efficiency of the initial DA reaction, each of the CPD derivatives (1.3 equiv) were heated with Pe-NBD-OH (1.0 equiv, 0.5 M in toluene) at 70 °C. After 21 h, ^{1}H NMR of the crude reaction mixtures indicated the formation of Ph-NBD−CPD, Me-CPD−NBD, and B-CPD−NBD to be 7, 16, and >98%, respectively. From this series, B-CPD proved to be an excellent candidate as the DA is observed to be near-quantitative. Presumably, the increase in aromaticity upon formation of a phenanthrene subunit within the fused ring system of B-CPD−NBD helped improve the efficiency of this reaction. Furthermore, we believe that sterics might also play a role; Me-CPD and B-CPD, both of which have reduced steric hindrance in comparison to the Ph-CPD analogue, were expected to undergo a more efficient cycloaddition with NBD. Of note, Me-CPD, which exists as a dimer,[53] required increased temperatures to promote the initial rDA between monomers and could be responsible for the lower yield of this derivative.

In an effort to improve yields of all adducts so that comparative studies could be conducted, separate optimized reaction conditions were identified for each CPD derivative. Heating Pe-NBD-OH at 75 °C with Ph-CPD (2.0 equiv) in chloroform for 5 days followed by removal of excess Ph-CPD through a plug of silica followed by crystallization from hexane afforded the product Ph-CPD−NBD in a modest 33% yield. In an attempt to further increase conversion and reduce the reaction time, the reaction temperature was increased to 85 °C. Thin-layer chromatography (TLC) of this reaction, however, indicated the formation of a nonpolar byproduct indicative of an unwanted thermal decarbonylation and cleavage to the substituted benzene. Similar challenges were observed for the preparation of Me-CPD−NBD when the reaction temperature was increased in an effort to promote the retro-DA between Me-CPD dimers. Again, as observed with the Ph-CPD−NBD adduct, increased reaction temperature resulted in a nonpolar byproduct, indicating thermal decomposition of Me-CPD−NBD. Thermal decomposition of these adducts was further confirmed by ^{1}H NMR spectroscopy of the isolated nonpolar byproducts, indicating the production of Ph-benzene and Me-benzene. Despite these challenges, optimized conditions, heating Pe-NBD-OH at 85 °C with Me-CPD (1.5 equiv) in toluene for 24 h, improved the overall yield of Me-CPD-NBD from 17 to 42%. Additionally, the purposeful thermal decomposition of Ph-CPD−NBD and Me-CPD−NBD by refluxing in toluene as described in the Supporting Information provided an efficient route to the substituted benzenes for subsequent UV−vis studies. Finally, it was found that the equivalents of B-CPD and reaction time could be reduced to 1.1 and 18 h, respectively. This optimized procedure afforded

https://doi.org/10.1021/acsami.1c08670
ACS Appl. Mater. Interfaces 2021, 13, 35422−35430

B-CPD−NBD in an 81% yield and only required filtration of the reaction mixture to obtain the purified material. Optimized reaction conditions and isolated yields for the three adducts are reported in Figure 1a, and full synthetic details for each compound can be found in the Supporting Information.

2.1.2. Thermal Stability of CPD−NBD Adducts. For the desired application of these adducts in photopatterning, the competing thermal decarbonylation of CPD−NBD adducts[49,52] must be avoided as it could result in nonselective, off-target DA reactions with maleimides. Furthermore, adduct stability would directly impact the long-term storage of these materials before patterning or the ability to invoke additional processing steps. Our initial investigation into the synthesis of these three adducts indicated that for Ph-CPD−NBD and Me-CPD−NBD, the thermal stabilities were relatively low as byproducts were observed upon prolonged heating in solution at 85 °C. To systematically compare the thermal stability of the three adducts, thermogravimetric analysis (TGA) coupled with evolved gas analysis (EGA) by mass spectrometry was used. For Ph-CPD−NBD and Me-CPD−NBD, the adducts are shown to undergo thermal decomposition around 170 °C (Figure 1b); however, CO detection is observed starting at 156 and 152 °C for the two adducts, respectively (Figures S27 and S28). Notably, B-CPD−NBD shows a significantly improved thermal stability requiring an additional 50 °C for CO release (Figure 1b). This is in good agreement with literary reports of heating such fused adducts,[49,62] although thorough thermal analysis has not been reported.

2.1.3. Photodecarbonylation Studies. To probe the viability of each CPD−NBD adduct as a photolabile Cp precursor, 25 μM solutions of each adduct were prepared and monitored by ^{1}H NMR while irradiated in a Rayonet RPR-200 chamber (300 nm). Irradiation was performed directly in sealed, nitrogen-sparged NMR tubes to avoid the formation of oxidized byproducts.[51,52] The initial rate of Cp production was highest for B-CPD−NBD, although a notable reduction in the rate is observed over the course of the reaction (Figure 1c). This was attributed to the increase in the absorbance of the fused ring system of the liberated B-benzene byproduct leading to product inhibition. This was confirmed by UV−vis spectroscopy, which revealed an increase in molar absorptivity at 300 nm from 9100 M^{-1} cm^{-1} of B-CPD−NBD to 27 000 M^{-1} cm^{-1} of B-benzene (Table 1 and Figures S40−S42). Additionally, irradiation of 25 μM B-CPD−NBD solutions doped with either 0.2 or 0.5 equiv of B-benzene slowed the rate of photodecarbonylation (Figure S33), further corroborating our assumption. It is possible that shorter wavelengths might offer a solution to the observed product inhibition, but the increased likelihood of degradation and the desire to present a mild patterning platform motivated us to move forward with long-wave UV irradiation.

Table 1. Photophysical Properties of Adducts and Substituted Benzene Byproducts

	$\varepsilon_{max,\ 212\ nm}$ (M^{-1} cm^{-1})	$\varepsilon_{300\ nm}$ (M^{-1} cm^{-1})	Φ (%)
Ph-CPD−NBD	120 000	7800	2.8 ± 0.4
Me-CPD−NBD	19 000	2200	2.5 ± 0.3
B-CPD−NBD	39 000	9100	5.3 ± 0.8
Ph-benzene	100 000	1900	
Me-benzene	20 000	180	
B-benzene	59 000	27 000	

To quantify the efficiency of the photoinduced production of cyclopentadiene from the three CPD−NBD adducts, quantum yields were determined at low conversions (<15%). In agreement with the initial monitoring study, the quantum yield of B-CPD-NBD was twice that of the two nonfused derivatives (Table 1, entry 3). In spite of the minor product inhibition observed at 300 nm for B-CPD−NBD, we were pleased to see significant liberation of Cp upon irradiation and encouraged by its facile synthesis and superior thermal stability. This adduct was taken forward in two polymer networks to demonstrate its potential as a photopatterning platform via spatially controlled diene liberation and subsequent DA reactions.

2.2. Preparation and Patterning of Polymer Networks. *2.2.1. Preparation of Polyacrylate Networks.* To highlight the potential of this photoinduced cleavage as a patterning platform, we first sought to incorporate the adduct using a traditional acrylate free-radical polymerization. An acrylate monomer was prepared from B-CPD−NBD in one step (Figure 2a). Drawing from photopolymerization methods used to construct thin networks, glass cells were prepared of 50 μm thickness and infiltrated with a neat monomer mixture of B-CPD−NBD acrylate, butyl acrylate, and 1,4-butanediol diacrylate. The visible light photoinitiator, phenylbis(2,4,6-trimethylbenzoyl)phosphine oxide (BAPO), was employed to allow for photopolymerization at 405 nm and avoid unwanted decarbonylation of the incorporated CPD−NBD adducts during network formation. After photopolymerization, the poly(butyl acrylate) (PBA) films were removed from the glass cells and taken forward in patterning studies. The second type of PBA network was also prepared using Diels−Alder chemistry to cross-link tetra-PBA polymers, which also exhibited successful patterning (Figure S49).

2.2.2. Decarbonylation within Polymer Networks. We reasoned that the detection of carbon monoxide during irradiation of polymer thin films would offer a facile approximation of conversion. Numerous methods exist for the efficient detection of CO, particularly from the field of therapeutic CO-releasing systems.[55,63−65] Inspired by the use of commercially available CO detectors by several groups,[64,65] a small closed system equipped with a CO sensor purchased from SPEC sensors was prepared (Product No. 110-102; Figure S50). This simple CO detector allowed for the monitoring of CO production in neat samples of B-CPD−NBD (Figure S51) or within polymer networks (Figure 2b). Similar to the ^{1}H NMR study demonstrated in Figure 1c, the initial rate slows due to product inhibition by B-benzene, and after 240 min of irradiation, the concentration of CO remains constant. With this in mind, subsequent patterning studies were irradiated between 30 and 240 min before treatment with the desired maleimide and assumed to result in a 50−70% conversion followed by near-quantitative clicking to the maleimide of choice. These irradiation times are comparable to the 3 h irradiation reported for the photodecarbonylation of CPD−maleimide adducts[37] and presumably could be shortened to cytocompatible light doses (<10 min)[66] if complete photodeprotection is not necessary.

2.2.3. Poly(butyl acrylate) Network Patterning with Dyes. Selective photoinduced liberation of Cp was visually confirmed by irradiating the networks with a collimated LED (Thorlabs, 365 nm, 6.1 mW/cm^2) through a simple quartz photomask

https://doi.org/10.1021/acsami.1c08670
ACS Appl. Mater. Interfaces 2021, 13, 35422−35430

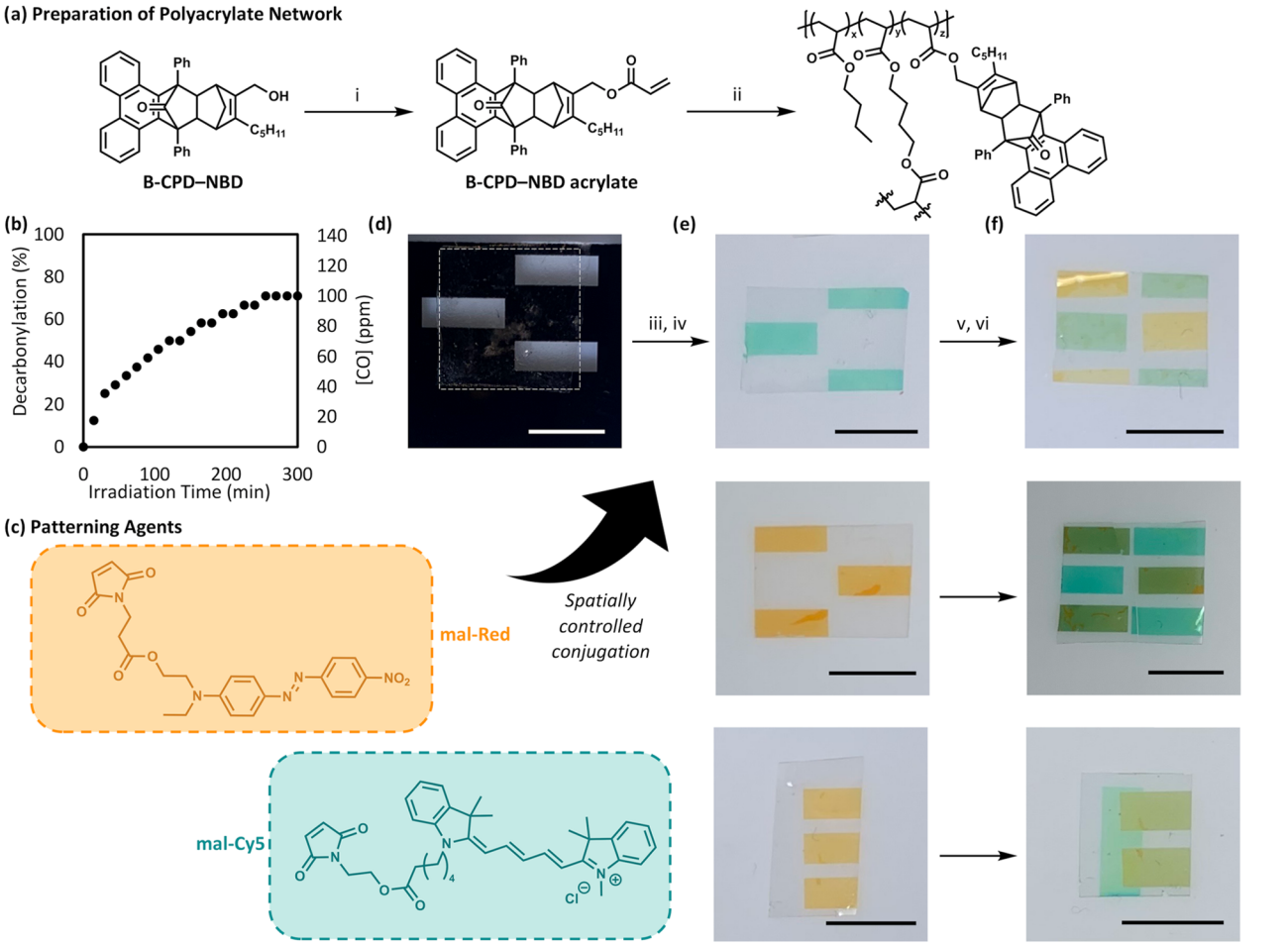

Figure 2. (a) (i) Acryloyl chloride (1.5 equiv), Et_3N (1.5 equiv), DCM, 0 °C, 4 h, 80%. (ii) Butyl acrylate (74 mol %), 1,4-butanediol diacrylate (20 mol %), B-CPD−NBD acrylate (5 mol %), BAPO (1 mol %), 405 nm, 30 min, rt. (b) Monitoring by CO sensor upon irradiation with 365 nm LED, plotted against ppm CO and calculated reaction completion. (c) Structures of maleimide-functionalized dyes. (d) Photograph of quartz photomask used for patterning films with a nonpatterned film outlined in white. (iii) 365 nm, 6.1 mW/cm^2, 30 min. (iv) mal-Cy5 (10 mM in DCM), 1 h. (e) Photographs of films after initial patterning. (v) 365 nm, 6.1 mW/cm^2, 30 min. (vi) mal-Red (10 mM in DCM), 1 h. (f) Photographs of films after second patterning step. Scale bars = 5 mm.

(Figure 2d) and then swelling in solutions of dichloromethane (DCM) containing maleimide dyes. Of note, efficient patterning is observed using long-range UV light (365 nm), and irradiation of films performed in air provided qualitatively similar results in dye pattern compared to that in a nitrogen-purged vessel (Figure S53). Although quantification of possible oxidized byproducts[51,52] could not be performed in the thin film, successful patterning without the exclusion of oxygen indicated minimal interference of these byproducts and prompted subsequent patterning studies to be performed using 365 nm irradiation and open to air to highlight the synthetic ease and mild nature of this patterning platform. Additionally, due to the incorporation of a persistent diene into the resulting polymer network, patterning did not require in situ trapping or immediate post-treatment with a maleimide; in fact, successful dye conjugation could be achieved by treating the materials with maleimides several hours post irradiation. We predict that patterning could be achieved with longer gaps between irradiation and maleimide treatment but did not investigate longer time scales so as to avoid the potential of cyclopentadiene dimerization within the network.

Here, we demonstrate the ability to pattern two highly absorbing dyes, maleimide-disperse red 1 (mal-Red) and maleimide-cyanine 5 (mal-Cy5) in predetermined locations within a single polymer network. To prepare the multi-patterned material, films were irradiated under a quartz photomask for 30 min before swelling in a solution of either mal-Red or mal-Cy5. The material was rinsed with DCM to remove the nonconjugated dye, affording the patterned thin films depicted in Figure 2e. A second pattern could be programmed into the films by irradiation with a second, inverted quartz photomask for 30 min, followed by treatment with a 10 mM solution of the alternative dye in DCM for 2 h. Rinsing to remove the residual dye afforded multispecies-patterned thin films (Figure 2f). It is worth noting that after the second patterning step, both dyes were consistently observed in locations of the first pattern, resulting in a green tint. This could be due to an interaction between the two dyes or clicking to Cp not consumed during the first dye treatment. A control experiment was performed by treating a Cy5-patterned film with commercially available disperse red 1, which did not contain the maleimide click functional group. Again, the staining was observed (Figure S54), indicating that the cause of this is most likely an interaction of the two dyes rather than incomplete conversion of the initially exposed Cp units. That being said, we were quite pleased with the

https://doi.org/10.1021/acsami.1c08670
ACS Appl. Mater. Interfaces 2021, 13, 35422−35430

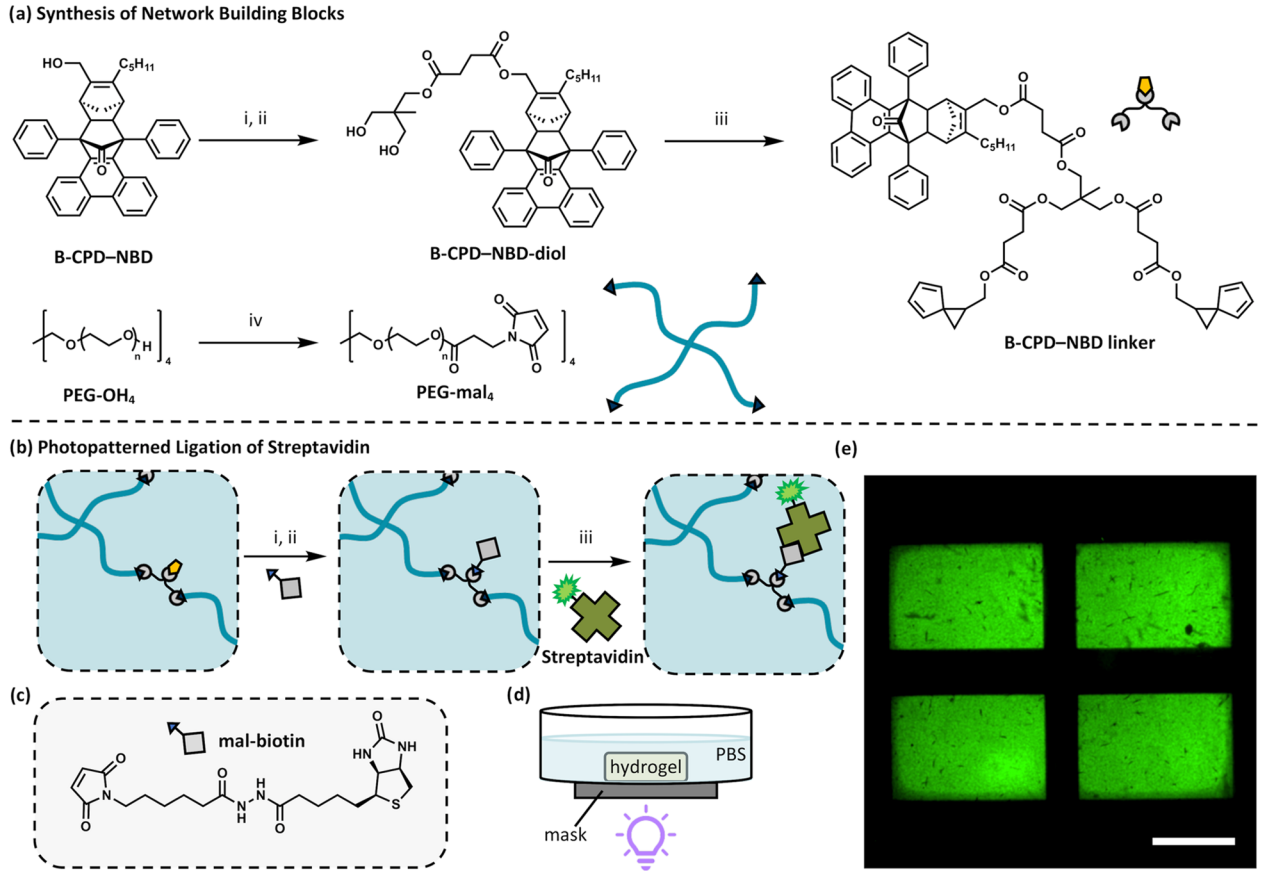

Figure 3. (a) (i) Succinic anhydride (1.3 equiv), triethylamine (1.0 equiv), 4-dimethylaminopyridine (DMAP, 0.1 equiv), dichloromethane (DCM), 1 h, 81%; (ii) trimethylolethane (4.0 equiv), *N*-(3-dimethylaminopropyl)-*N*′-ethylcarbodiimide hydrochloride (EDC, 1.5 equiv), DMAP (0.1 equiv), *N*,*N*-dimethylformamide, rt, 3 h, 58%; (iii) spiro[2.4]hepta-4,6-diene-COOH (3.0 equiv), EDC (3.0 equiv), DMAP (0.2 equiv), DCM, rt, 1.5 h, 92%; (iv) 3-maleimidopropanoic acid (10.0 equiv), N,N′-dicyclohexylcarbodiimide (11.0 equiv), DMAP (0.1 equiv), DCM, rt, 24 h. (b) Schematic representation of the maleimide–biotin photoclick, followed by streptavidin ligation. (i) 365 nm, PBS, 6.1 mW/cm^2, 30 min; (ii) mal–biotin (1 mg/mL in 9:1 PBS, DMSO), 2 h; (iii) streptavidin–Alexa Fluor 514 conjugate (100 μL of 0.5 mg/mL in PBS dropped onto hydrogel), dark, 1 h. (c) Structure of maleimide-functionalized biotin. (d) Schematic representation of the hydrogel photopatterning setup. (e) Fluorescence image of the resulting hydrogel with the patterned ligation of the streptavidin–Alexa Fluor 514 conjugate. Multiple images were stitched due to the limited field of view. Scale bar = 1.5 mm.

resolution achieved and simplicity of the patterning and believe that this procedure will be compatible with a variety of diene-functionalized species.

2.2.4. Hydrogel Patterning with Biotin and Streptavidin. To test the versatility of this platform, we next sought to apply the patterning technique to achieve preprogrammed protein immobilization in biocompatible PEG hydrogels. A functional linker was designed to incorporate B-CPD–NBD units into tetra-PEG-based hydrogels, and as an additional testament to the utility of DA click chemistry, we chose to prepare the hydrogels themselves via DA cycloadditions. Commercially available tetra-PEG (M_n = 20 000 g/mol) was functionalized with maleimide by modifying a reported carbodiimide coupling[48] (PEG-mal$_4$, $M_{n(HNMR)}$ = 21 700 g/mol; Figures 3a, S21, and S22). Spiro[2.4]hepta-4,6-diene was chosen as the diene partner for the initial network formation due to its efficient DA reactivity,[29] while the inhibition of the dimerization leads to improved monomer stability.[67] A diene-functionalized linker (B-CPD–NBD linker) was prepared in three steps from B-CPD–NBD (Figure 3a). Due to the insolubility of the B-CPD–NBD linker in water, the polymer network was prepared by combining PEG-mal$_4$ and B-CPD–NBD linker in dimethyl sulfoxide (DMSO) (10 wt % polymer) and then drop-casting 100 μL into a glass dish with a 10 mm diameter well (1 mm depth). Upon network formation, the network was washed and incubated in phosphate-buffered saline (PBS) before irradiation and patterning.

The well-containing glass dish allowed for bottom-up irradiation of the hydrogel while swollen in PBS (Figure 3d). After irradiation, the hydrogel was incubated in a PBS/DMSO solution containing mal–biotin. The resulting functionalized hydrogel was then rinsed with methanol and PBS to remove the nonconjugated mal–biotin. To offer a visual demonstration, the spatially biotinylated hydrogel was incubated with a solution containing streptavidin–Alexa Fluor 514 conjugate for 1 h in the dark (Figure 3b). The hydrogel was rinsed thoroughly with PBS to remove the nonligated protein before examination by fluorescence microscopy. Detection of Alexa Fluor 514 revealed selective protein immobilization onto the hydrogel corresponding to the predetermined photopattern (Figures 3c and S56). Furthermore, Z-stacks through the thickness of the sample reveal a strong Alexa Fluor 514 fluorescence signal throughout the sample thickness (Figures S55 and S57), highlighting effective penetration and high efficiency of this hydrogel functionalization strategy.

https://doi.org/10.1021/acsami.1c08670
ACS Appl. Mater. Interfaces 2021, 13, 35422–35430

3. CONCLUSIONS

A new Diels–Alder photoclick platform has been developed utilizing spatially controlled, on-demand unveiling of Cp in preformed polymer networks. Notably, due to the formation of a stable diene that does not require in situ trapping, maleimides can be clicked post irradiation. This allows access to functionalization with the cyanine dye utilized here, which is highly susceptible to bleaching by photo-oxidation.[68,69] We envision that this patterning procedure could be used directly for the multispecies patterning of a multitude of materials and is particularly useful in patterning photothermal and photoresponsive units, which are incompatible with the traditional in situ photoclicking reactions currently available. Furthermore, the ability to conjugate multiple absorbing species, as we have demonstrated with cyanine 5 and disperse red 1, offers exciting potential in sequential, wavelength-controlled responses in smart materials. Mild, efficient, bio-orthogonal chemistry also provides promise for use in biomaterials. The simple biotin–streptavidin protein ligation presented serves as a proof-of-concept, but the success of this platform within a biocompatible system and the use of a cytocompatible light source[66] validates the promise of this system within biological systems. Specifically, the spatially controlled functionalization of synthetic and naturally derived hydrogels could offer a means of studying the effect of heterogeneous physical or biochemical cues on cell behavior. Given the success of the two patterning applications debuted here and the promise within a range of next-generation materials including sequentially stimuli-responsive polymers and spatially controlled cellular microenvironments, we believe that this platform will offer a convenient and ubiquitous patterning method with numerous advantages over current systems.

4. EXPERIMENTAL SECTION

4.1. Synthetic Methods. All chemicals were obtained from Sigma-Aldrich, TCI Europe, or Fisher Scientific. Reagent-grade solvents were stored over 3 Å molecular sieves prior to use, and unless otherwise noted, all reagents were used as received without further purification. Thin-layer chromatography (TLC) was conducted with E. Merck silica gel 60 F254 precoated plates (0.25 mm) and visualized by exposure to UV light (254 nm) or stained with *p*-anisaldehyde. Flash column chromatography was performed using normal phase silica gel (60 Å, 0.040–0.063 mm, Geduran) with hexanes, ethyl acetate, dichloromethane, and/or methanol as eluents. Full synthetic detail and characterization of CPD–NBD adducts and network building blocks can be found in the Supporting Information.

4.2. Analysis of CPD–NBD Adducts. Thermogravimetric analysis (TGA) and mass spectra were collected on a TA Instruments Discovery Thermo-Gravimetric Analyzer with mass spectrometer assembly. The measurements were performed under a nitrogen environment from room temperature ramping up to 300 °C at 20 °C/min, and the evolved gas was analyzed for 28 amu corresponding to the decarbonylation event for each adduct (Figures S27–S29). Photodecarbonylation studies to confirm the production of cyclopentadiene and determine quantum yields were performed using a Rayonet RPR-200 chamber (300 nm), and ^{1}H NMR spectra were recorded on a Varian spectrometer (600 MHz). For determination of quantum yields, potassium ferrioxalate was used as the actinometer (Figures S45–S48).[70] Quantitative ^{1}H NMR spectra were recorded with a relaxation delay of 20 s and a pulse width of 90°, and reaction conversion was calculated from the ratio of integrals from the product proton signals against ethylene carbonate internal standard. UV–vis absorption spectra were recorded on an Agilent 8453 UV–vis spectrometer from 190 to 1100 nm.

4.3. Fluorescence Microscopy. Patterned streptavidin immobilization was visualized with a spinning disc super-resolution confocal microscope (Nikon) with a 4× lens. Images were captured with a 100 ms exposure of a 488 nm laser (75%). Z-stacks, to measure pattern penetration, were taken every 12.5 μm for 1.6 mm with the same imaging settings and quantified with the *Plot Z axis Profile* function in FIJI.

■ ASSOCIATED CONTENT

Supporting Information

The Supporting Information is available free of charge at https://pubs.acs.org/doi/10.1021/acsami.1c08670.

Further information regarding synthetic procedures, characterization, instrumentation, and data is not included in the main text (PDF)

■ AUTHOR INFORMATION

Corresponding Author

Javier Read de Alaniz – *Department of Chemistry and Biochemistry, University of California, Santa Barbara, Santa Barbara, California 93106, United States;* orcid.org/0000-0003-2770-9477; Email: javier@chem.ucsb.edu

Authors

Sophia J. Bailey – *Department of Chemistry and Biochemistry, University of California, Santa Barbara, Santa Barbara, California 93106, United States*

Friedrich Stricker – *Department of Chemistry and Biochemistry, University of California, Santa Barbara, Santa Barbara, California 93106, United States*

Erik Hopkins – *Department of Molecular, Cellular, and Developmental Biology, University of California, Santa Barbara, Santa Barbara, California 93106, United States*

Maxwell Z. Wilson – *Department of Molecular, Cellular, and Developmental Biology, University of California, Santa Barbara, Santa Barbara, California 93106, United States;* orcid.org/0000-0002-2806-1919

Complete contact information is available at: https://pubs.acs.org/10.1021/acsami.1c08670

Author Contributions

The manuscript was written by S.J.B. and J.R.d.A. and revised by S.J.B., J.R.d.A., and F.S. Experiments were designed by S.J.B. and J.R.d.A. S.J.B., F.S., and E.H. performed the experiments. All authors have given approval to the final version of the manuscript.

Notes

The authors declare no competing financial interest.

■ ACKNOWLEDGMENTS

This research was partially supported by the Office of Naval Research through the MURI of Photomechanical Materials Systems (ONR N00014-18-1-2624) and partially supported by the BioPACIFIC Materials Innovation Platform of the National Science Foundation under Award No. DMR-1933487. S.J.B. and E.H. would also like to thank the BioPACIFIC MIP for financial support, mentorship, and collaboration opportunities as BioPACIFIC Fellows. S.J.B. thanks the UCSB graduate division for financial support through a Chancellor's Fellowship. In addition, the authors would also like to thank the staff of the UC Santa Barbara Mass Spectrometry Facility and TEMPO Facility within the Materials Research Laboratory (MRL) for assisted data

acquisition during shutdowns related to the COVID-19 pandemic.

■ ABBREVIATIONS

DA, Diels−Alder
IEDDA, inverse electron demand DA
rDA, retro DA
Cp, cyclopentadiene
mal, maleimide
CPD−NBD, cyclopentadienone−norbornadiene
PEG, poly(ethylene glycol)
PBS, phosphate-buffered saline

■ REFERENCES

(1) Zhang, W.; Wang, R.; Sun, Z.; Zhu, X.; Zhao, Q.; Zhang, T.; Cholewinski, A.; Yang, F.; Zhao, B.; Pinnaratip, R.; Forooshani, P. K.; Lee, B. P. Catechol-Functionalized Hydrogels: Biomimetic Design, Adhesion Mechanism, and Biomedical Applications. *Chem. Soc. Rev.* **2020**, *49*, 433−464.
(2) Vermonden, T.; Censi, R.; Hennink, W. E. Hydrogels for Protein Delivery. *Chem. Rev.* **2012**, *112*, 2853−2888.
(3) Zhu, J. Bioactive Modification of Poly(Ethylene Glycol) Hydrogels for Tissue Engineering. *Biomaterials* **2010**, *31*, 4639−4656.
(4) Küpfer, J.; Finkelmann, H. Nematic Liquid Single Crystal Elastomers. *Makromol. Chem., Rapid Commun.* **1991**, *12*, 717−726.
(5) Ge, F.; Yang, R.; Tong, X.; Camerel, F.; Zhao, Y. A Multifunctional Dye-Doped Liquid Crystal Polymer Actuator: Light-Guided Transportation, Turning in Locomotion, and Autonomous Motion. *Angew. Chem.* **2018**, *130*, 11932−11937.
(6) Francis, W.; Dunne, A.; Delaney, C.; Florea, L.; Diamond, D. Spiropyran Based Hydrogels Actuators—Walking in the Light. *Sens. Actuators, B* **2017**, *250*, 608−616.
(7) Lahikainen, M.; Kuntze, K.; Zeng, H.; Helanterä, S.; Hecht, S.; Priimagi, A. Tunable Photomechanics in Diarylethene-Driven Liquid Crystal Network Actuators. *ACS Appl. Mater. Interfaces* **2020**, *12*, 47939−47947.
(8) Gelebart, A. H.; Mulder, D. J.; Vantomme, G.; Schenning, A. P. H. J.; Broer, D. J. A Rewritable, Reprogrammable, Dual Light-Responsive Polymer Actuator. *Angew. Chem., Int. Ed.* **2017**, *56*, 13436−13439.
(9) Liu, Y.; Shaw, B.; Dickey, M. D.; Genzer, J. Sequential Self-Folding of Polymer Sheets. *Sci. Adv.* **2017**, *3*, No. e1602417.
(10) Lahikainen, M.; Zeng, H.; Priimagi, A. Design Principles for Non-Reciprocal Photomechanical Actuation. *Soft Matter* **2020**, *16*, 5951−5958.
(11) DeForest, C. A.; Polizzotti, B. D.; Anseth, K. S. Sequential Click Reactions for Synthesizing and Patterning Three-Dimensional Cell Microenvironments. *Nat. Mater.* **2009**, *8*, 659−664.
(12) DeForest, C. A.; Tirrell, D. A. A Photoreversible Protein-Patterning Approach for Guiding Stem Cell Fate in Three-Dimensional Gels. *Nat. Mater.* **2015**, *14*, 523−531.
(13) Batalov, I.; Stevens, K. R.; DeForest, C. A. Photopatterned Biomolecule Immobilization to Guide Three-Dimensional Cell Fate in Natural Protein-Based Hydrogels. *Proc. Natl. Acad. Sci. U.S.A.* **2021**, *118*, No. e2014194118.
(14) Kolb, H. C.; Finn, M. G.; Sharpless, K. B. Click Chemistry: Diverse Chemical Function from a Few Good Reactions. *Angew. Chem., Int. Ed.* **2001**, *40*, 2004−2021.
(15) Rostovtsev, V. V.; Green, L. G.; Fokin, V. V.; Sharpless, K. B. A Stepwise Huisgen Cycloaddition Process: Copper(I)-Catalyzed Regioselective "Ligation" of Azides and Terminal Alkynes. *Angew. Chem., Int. Ed.* **2002**, *41*, 2596−2599.
(16) Nair, D. P.; Podgórski, M.; Chatani, S.; Gong, T.; Xi, W.; Fenoli, C. R.; Bowman, C. N. The Thiol-Michael Addition Click Reaction: A Powerful and Widely Used Tool in Materials Chemistry. *Chem. Mater.* **2014**, *26*, 724−744.
(17) Hoyle, C. E.; Bowman, C. N. Thiol-Ene Click Chemistry. *Angew. Chem., Int. Ed.* **2010**, *49*, 1540−1573.
(18) Kose, M. M.; Yesilbag, G.; Sanyal, A. Segment Block Dendrimers via Diels−Alder Cycloaddition. *Org. Lett.* **2008**, *10*, 2353−2356.
(19) Inglis, A. J.; Sinnwell, S.; Stenzel, M. H.; Barner-Kowollik, C. Ultrafast Click Conjugation of Macromolecular Building Blocks at Ambient Temperature. *Angew. Chem., Int. Ed.* **2009**, *48*, 2411−2414.
(20) Billiet, S.; De Bruycker, K.; Driessen, F.; Goossens, H.; Van Speybroeck, V.; Winne, J. M.; Du Prez, F. E. Triazolinediones Enable Ultrafast and Reversible Click Chemistry for the Design of Dynamic Polymer Systems. *Nat. Chem.* **2014**, *6*, 815−821.
(21) Hansell, C. F.; Espeel, P.; Stamenović, M. M.; Barker, I. A.; Dove, A. P.; Du Prez, F. E.; O'Reilly, R. K. Additive-Free Clicking for Polymer Functionalization and Coupling by Tetrazine−Norbornene Chemistry. *J. Am. Chem. Soc.* **2011**, *133*, 13828−13831.
(22) St Amant, A. H.; Discekici, E. H.; Bailey, S. J.; Zayas, M. S.; Song, J.-A.; Shankel, S. L.; Nguyen, S. N.; Bates, M. W.; Anastasaki, A.; Hawker, C. J.; Read de Alaniz, J. Norbornadienes: Robust and Scalable Building Blocks for Cascade "Click" Coupling of High Molecular Weight Polymers. *J. Am. Chem. Soc.* **2019**, *141*, 13619−13624.
(23) Samoshin, A. V.; Hawker, C. J.; Read de Alaniz, J. Nitrosocarbonyl Hetero-Diels−Alder Cycloaddition: A New Tool for Conjugation. *ACS Macro Lett.* **2014**, *3*, 753−757.
(24) Chen, X.; Wudl, F.; Mal, A. K.; Shen, H.; Nutt, S. R. New Thermally Remendable Highly Cross-Linked Polymeric Materials. *Macromolecules* **2003**, *36*, 1802−1807.
(25) Murphy, E. B.; Bolanos, E.; Schaffner-Hamann, C.; Wudl, F.; Nutt, S. R.; Auad, M. L. Synthesis and Characterization of a Single-Component Thermally Remendable Polymer Network: Staudinger and Stille Revisited. *Macromolecules* **2008**, *41*, 5203−5209.
(26) Liu, Y.-L.; Chuo, T.-W. Self-Healing Polymers Based on Thermally Reversible Diels−Alder Chemistry. *Polym. Chem.* **2013**, *4*, 2194.
(27) Blackman, M. L.; Royzen, M.; Fox, J. M. Tetrazine Ligation: Fast Bioconjugation Based on Inverse-Electron-Demand Diels−Alder Reactivity. *J. Am. Chem. Soc.* **2008**, *130*, 13518−13519.
(28) Oliveira, B. L.; Guo, Z.; Bernardes, G. J. L. Inverse Electron Demand Diels−Alder Reactions in Chemical Biology. *Chem. Soc. Rev.* **2017**, *46*, 4895−4950.
(29) St Amant, A. H.; Lemen, D.; Florinas, S.; Mao, S.; Fazenbaker, C.; Zhong, H.; Wu, H.; Gao, C.; Christie, R. J.; Read de Alaniz, J. Tuning the Diels−Alder Reaction for Bioconjugation to Maleimide Drug-Linkers. *Bioconjugate Chem.* **2018**, *29*, 2406−2414.
(30) Kumar, A.; Mao, S.; Dimasi, N.; Gao, C. Design and Validation of Linkers for Site-Specific Preparation of Antibody−Drug Conjugates Carrying Multiple Drug Copies Per Cysteine Conjugation Site. *Int. J. Mol. Sci.* **2020**, *21*, No. 6882.
(31) Smith, L. J.; Taimoory, S. M.; Tam, R. Y.; Baker, A. E. G.; Binth Mohammad, N.; Trant, J. F.; Shoichet, M. S. Diels−Alder Click-Cross-Linked Hydrogels with Increased Reactivity Enable 3D Cell Encapsulation. *Biomacromolecules* **2018**, *19*, 926−935.
(32) Yang, N. C.; Rivas, C. A New Photochemical Primary Process, the Photochemical Enolization of *o*-Substituted Benzophenones. *J. Am. Chem. Soc.* **1961**, *83*, 2213.
(33) Meador, M. A. B.; Meador, M. A.; Williams, L. L.; Scheiman, D. A. Diels−Alder Trapping of Photochemically Generated Dienes with a Bismaleimide: A New Approach to Polyimide Synthesis. *Macromolecules* **1996**, *29*, 8983−8986.
(34) Gruendling, T.; Oehlenschlaeger, K. K.; Frick, E.; Glassner, M.; Schmid, C.; Barner-Kowollik, C. Rapid UV Light-Triggered Macromolecular *Click* Conjugations via the Use of *o* -Quinodimethanes. *Macromol. Rapid Commun.* **2011**, *32*, 807−812.
(35) Glassner, M.; Oehlenschlaeger, K. K.; Gruendling, T.; Barner-Kowollik, C. Ambient Temperature Synthesis of Triblock Copolymers via Orthogonal Photochemically and Thermally Induced Modular Conjugation. *Macromolecules* **2011**, *44*, 4681−4689.

https://doi.org/10.1021/acsami.1c08670
ACS Appl. Mater. Interfaces 2021, 13, 35422−35430

(36) Pauloehrl, T.; Delaittre, G.; Winkler, V.; Welle, A.; Bruns, M.; Börner, H. G.; Greiner, A. M.; Bastmeyer, M.; Barner-Kowollik, C. Adding Spatial Control to Click Chemistry: Phototriggered Diels-Alder Surface (Bio)Functionalization at Ambient Temperature. *Angew. Chem., Int. Ed.* **2012**, *51*, 1071−1074.
(37) Pauloehrl, T.; Welle, A.; Bruns, M.; Linkert, K.; Börner, H. G.; Bastmeyer, M.; Delaittre, G.; Barner-Kowollik, C. Spatially Controlled Surface Immobilization of Nonmodified Peptides. *Angew. Chem., Int. Ed.* **2013**, *52*, 9714−9718.
(38) Tischer, T.; Claus, T. K.; Bruns, M.; Trouillet, V.; Linkert, K.; Rodriguez-Emmenegger, C.; Goldmann, A. S.; Perrier, S.; Börner, H. G.; Barner-Kowollik, C. Spatially Controlled Photochemical Peptide and Polymer Conjugation on Biosurfaces. *Biomacromolecules* **2013**, *14*, 4340−4350.
(39) Arumugam, S.; Popik, V. V. Light-Induced Hetero-Diels−Alder Cycloaddition: A Facile and Selective Photoclick Reaction. *J. Am. Chem. Soc.* **2011**, *133*, 5573−5579.
(40) Frazier, C. P.; Palmer, L. I.; Samoshin, A. V.; Read de Alaniz, J. Accessing Nitrosocarbonyl Compounds with Temporal and Spatial Control via the Photoredox Oxidation of N-Substituted Hydroxylamines. *Tetrahedron Lett.* **2015**, *56*, 3353−3357.
(41) Glassner, M.; Oehlenschlaeger, K. K.; Welle, A.; Bruns, M.; Barner-Kowollik, C. Polymer Surface Patterningvia Diels−Alder Trapping of Photo-Generated Thioaldehydes. *Chem. Commun.* **2013**, *49*, 633−635.
(42) Lemieux, V.; Gauthier, S.; Branda, N. R. Selective and Sequential Photorelease Using Molecular Switches. *Angew. Chem.* **2006**, *118*, 6974−6978.
(43) Erno, Z.; Asadirad, A. M.; Lemieux, V.; Branda, N. R. Using Light and a Molecular Switch to 'Lock' and 'Unlock' the Diels−Alder Reaction. *Org. Biomol. Chem.* **2012**, *10*, 2787.
(44) Kumar, G. S.; Lin, Q. Light-Triggered Click Chemistry. *Chem. Rev.* **2021**, *121*, 6991−7031.
(45) Sauer, J.; Lang, D.; Mielert, A. The Order of Reactivity of Dienes towards Maleic Anhydride in the Diels-Alder Reaction. *Angew. Chem., Int. Ed.* **1962**, *1*, 268−269.
(46) Inglis, A. J.; Paulöhrl, T.; Barner-Kowollik, C. Ambient Temperature Synthesis of a Versatile Macromolecular Building Block: Cyclopentadienyl-Capped Polymers. *Macromolecules* **2010**, *43*, 33−36.
(47) Levandowski, B. J.; Raines, R. T. Click Chemistry with Cyclopentadiene. *Chem. Rev.* **2021**, *121*, 6777−6801.
(48) Bailey, S. J.; Discekici, E. H.; Barbon, S. M.; Nguyen, S. N.; Hawker, C. J.; Read de Alaniz, J. Norbornadiene Chain-End Functional Polymers as Stable, Readily Available Precursors to Cyclopentadiene Derivatives. *Macromolecules* **2020**, *53*, 4917−4924.
(49) Mackenzie, K. 98. Bicyclo[2,2,1]Heptadiene in the Diels−Alder Reaction. *J. Chem. Soc.* **1960**, 473−483.
(50) Anderson, C. M.; Bremner, J. B.; Westberg, H. H.; Warrener, R. N. The Synthetic Potential of the 1,2-Photoaromatization (1) Reaction. *Tetrahedron Lett.* **1969**, *10*, 1585−1588.
(51) Wilson, W. S.; Warrener, R. N. Photodecarbonylation - a Gentle Route to Annelated Cyclohexadienes. *Tetrahedron Lett.* **1970**, *11*, 5203−5206.
(52) Findlay, D. M.; Roy, M. L.; McLean, S. Thermal Routes to Substituted Cyclopentadienes. *Can. J. Chem.* **1972**, *50*, 3186−3195.
(53) Ogliaruso, M. A.; Romanelli, M. G.; Becker, E. I. Chemistry of Cyclopentadienones. *Chem. Rev.* **1965**, *65*, 261−367.
(54) Fry, A. J.; Sherman, L. R.; Beaulieu, A. R.; Sherwin, C. The Reaction between 7-Oxanorbornadienes and Tetraarylcyclopentadienones: A Short Synthesis of 1,2,3,4-Tetraarylbenzenes. *J. Org. Chem.* **1990**, *55*, 389−391.
(55) Ji, X.; Zhou, C.; Ji, K.; Aghoghovbia, R. E.; Pan, Z.; Chittavong, V.; Ke, B.; Wang, B. Click and Release: A Chemical Strategy toward Developing Gasotransmitter Prodrugs by Using an Intramolecular Diels-Alder Reaction. *Angew. Chem., Int. Ed.* **2016**, *55*, 15846−15851.
(56) Ji, X.; Aghoghovbia, R. E.; De La Cruz, L. K. C.; Pan, Z.; Yang, X.; Yu, B.; Wang, B. Click and Release: A High-Content Bioorthogonal Prodrug with Multiple Outputs. *Org. Lett.* **2019**, *21*, 3649−3652.
(57) Dietrich, M.; Delaittre, G.; Blinco, J. P.; Inglis, A. J.; Bruns, M.; Barner-Kowollik, C. Photoclickable Surfaces for Profluorescent Covalent Polymer Coatings. *Adv. Funct. Mater.* **2012**, *22*, 304−312.
(58) Wang, Y.; Rivera Vera, C. I.; Lin, Q. Convenient Synthesis of Highly Functionalized Pyrazolines via Mild, Photoactivated 1,3-Dipolar Cycloaddition. *Org. Lett.* **2007**, *9*, 4155−4158.
(59) Michalek, L.; Krappitz, T.; Mundsinger, K.; Walden, S. L.; Barner, L.; Barner-Kowollik, C. Mapping Photochemical Reactivity Profiles on Surfaces. *J. Am. Chem. Soc.* **2020**, *142*, 21651−21655.
(60) Wilson, P. J.; Wells, J. H. The Chemistry and Utilization of Cyclopentadiene. *Chem. Rev.* **1944**, *34*, 1−50.
(61) Bertrand, G.; Wentrup, C. Nitrile Imines: From Matrix Characterization to Stable Compounds. *Angew. Chem., Int. Ed.* **1994**, *33*, 527−545.
(62) Rickborn, B. The Retro-Diels-Alder Reaction Part I. C−C Dienophiles. In *Organic Reactions*; John Wiley & Sons, Inc.: Hoboken, NJ, 1998; pp 1−393.
(63) Motterlini, R.; Clark, J. E.; Foresti, R.; Sarathchandra, P.; Mann, B. E.; Green, C. J. Carbon Monoxide-Releasing Molecules: Characterization of Biochemical and Vascular Activities. *Circ. Res.* **2002**, *90*, e17−e24.
(64) Hasegawa, U.; van der Vlies, A. J.; Simeoni, E.; Wandrey, C.; Hubbell, J. A. Carbon Monoxide-Releasing Micelles for Immunotherapy. *J. Am. Chem. Soc.* **2010**, *132*, 18273−18280.
(65) Bohlender, C.; Gläser, S.; Klein, M.; Weisser, J.; Thein, S.; Neugebauer, U.; Popp, J.; Wyrwa, R.; Schiller, A. Light-Triggered CO Release from Nanoporous Non-Wovens. *J. Mater. Chem. B* **2014**, *2*, 1454−1463.
(66) Bryant, S. J.; Nuttelman, C. R.; Anseth, K. S. Cytocompatibility of UV and Visible Light Photoinitiating Systems on Cultured NIH/3T3 Fibroblasts in Vitro. *J. Biomater. Sci., Polym. Ed.* **2000**, *11*, 439−457.
(67) Froese, R. D. J.; Organ, M. G.; Goddard, J. D.; Stack, T. D. P.; Trost, B. M. Theoretical and Experimental Studies of the Diels-Alder Dimerizations of Substituted Cyclopentadienes. *J. Am. Chem. Soc.* **1995**, *117*, 10931−10938.
(68) Byers, G. W.; Gross, S.; Henrichs, P. M. Direct And Sensitized Photooxidation Of Cyanine Dyes. *Photochem. Photobiol.* **1976**, *23*, 37−43.
(69) Gorka, A. P.; Schnermann, M. J. Harnessing Cyanine Photooxidation: From Slowing Photobleaching to near-IR Uncaging. *Curr. Opin. Chem. Biol.* **2016**, *33*, 117−125.
(70) Hatchard, C. G.; Parker, C. A.; Bowen, E. J. A New Sensitive Chemical Actinometer - II. Potassium Ferrioxalate as a Standard Chemical Actinometer. *Proc. R. Soc. A* **1956**, *235*, 518−536.

https://doi.org/10.1021/acsami.1c08670
ACS Appl. Mater. Interfaces 2021, 13, 35422−35430